We are IntechOpen,
the world's leading publisher of Open Access books
Built by scientists, for scientists

4,800
Open access books available

122,000
International authors and editors

135M
Downloads

Our authors are among the

154
Countries delivered to

TOP 1%
most cited scientists

12.2%
Contributors from top 500 universities

CLARIVATE ANALYTICS
BOOK CITATION INDEX
INDEXED

WEB OF SCIENCE™

Selection of our books indexed in the Book Citation Index
in Web of Science™ Core Collection (BKCI)

Interested in publishing with us?
Contact book.department@intechopen.com

Numbers displayed above are based on latest data collected.
For more information visit www.intechopen.com

Quantitative Planar Laser-Induced Fluorescence Technology

Zhen Yang, Xin Yu, Jiangbo Peng and
Jianlong Zhang

Additional information is available at the end of the chapter

Abstract

Planar laser-induced fluorescence (PLIF) is a highly sensitive and space-time-resolved laser diagnostic technique. It is widely used in the diagnosis of combustion and flow fields to obtain the thermodynamic information of active components and interested molecules in flames. Nowadays, the PLIF technology is developing in two directions: high speed and quantification. In view of the high spatial and temporal resolution characteristics of PLIF technology that other laser diagnostics do not possess, this chapter will focus on the basic principle of laser-induced fluorescence and the current research status of quantitative PLIF technology. In addition, the advantages and disadvantages of various quantitative technologies of component concentration in flames based on laser-induced fluorescence technology are analyzed. At last, the latest works on the quantification of species concentration using planar laser-induced fluorescence in combustion are introduced.

Keywords: bidirectional planar laser-induced fluorescence, combustion diagnostics, species concentration visualization, effective absorption cross section, laminar flames

1. Introduction

The planar laser-induced fluorescence [1] is a high-sensitivity and high-resolution laser spectral diagnostic technique developed in the 1980s. The emergence of PLIF technology has made great success in the visualization of the combustion field in flames, the dynamic evolution of the combustion process [2, 3], the temperature imaging [4, 5], and the quantitative measurements of the free radical concentrations under low pressure [6, 7]. PLIF technology is a noncontact measurement technology. Compared with the traditional contact measurement technology, PLIF technology not only has the unique advantages of noncontact and noninterference

to the combustion and flow fields but also can dynamically display and image two- or three-dimensional space structure of free radicals interested in combustion fields. These merits are unattainable and difficult to achieve by the traditional contact and other laser spectral diagnostic techniques, such as coherent anti-Stokes Raman scattering (CARS), degenerate four-wave mixing technology (DFWM), cavity ring down spectroscopy technology (CRDS), tunable diode laser absorption spectroscopy (TDLAS), and direct absorption spectroscopy.

Admittedly, PLIF technology also has its own shortcomings. The biggest obstacle is that the PLIF technology is rather difficult to achieve quantitative measurement. The greatest difficulty in quantification of the PLIF lies in the fact that the electronic collisional quenching rate of the molecules to be measured is not exactly the same at the different positions of flame under the normal and high pressures. Worse still, there is a big difference for the distribution of electronic quenching rates in different types of flames. In addition, the calibration factor is also a parameter, which is easy to change with the observation conditions. In a general way, the collisional quenching rates of the molecules to be measured in flame have little effect on the fluorescence signal under the low pressure, so it can be often neglected. However, the collisional quenching rates of molecules turn out to be very sensitive to the combustion environment in flames under normal and high pressures. Therefore, the profiles of the collisional quenching rates become difficult to be measured in real time due to the diversification of the flame structure. In this case, an additional consideration is needed to accurately deduce the concentration distribution information of the molecules to be measured using the fluorescence signals.

In order to eliminate the detrimental impact of quenching effect on the quantitative measurement of species concentration, Versluis et al. [8] proposed to combine the traditional laser-induced fluorescence (LIF) with absorption spectroscopy to excite the molecules using the two opposite direction laser beams, counteracting many influencing factors, such as collisional quenching effect, pressure, and the calibration constant of the Detector and optical system, so as to deduce species concentration profiles. However, the bidirectional LIF technology is highly depending on the spatial coincidence of the beam (especially for the sheet laser beam) and the signal-to-noise ratio (SNR) of the fluorescence signal, which leads to the lack of systematic research on this technology.

2. A brief analysis of planar laser-induced fluorescence

Laser-induced fluorescence is an essentially physical process of laser resonance excitation and fluorescence generation. When the molecule is excited by laser with a specific wavelength, it will transition from a low energy state (usually ground state) to a higher energy state (the excited state). Then the molecules in the excited state will spontaneously transition from the excited energy state to the low energy state after undergoing a series of non-radiative transition energy transfer. The energy of electromagnetic radiation between the excited state and the low energy state is released in the form of fluorescence radiation.

Hydroxyl (OH radical), a very important intermediate in flames, is considered to exist in the combustion process of most hydrocarbon fuels. Quantitative measurement of OH concentration

is of great significance for deep understanding, modification, and validation of reaction mechanism and chemical kinetic models. This chapter takes OH as an example to explain. Similar conclusions exist for other combustion intermediates or radicals.

The energy-level structure consists of the electronic, vibrational, and rotational energy levels. When numerous OH radicals in the flame absorb a certain wavelength laser from the ground state to the excited state, one part of molecules will shift to other vibrational or rotational energy levels due to the effect of vibrational energy transfer (VET) and rotational energy transfer (RET), one part of which will be transferred to the pre-dissociated state, and some of which will be quenched due to the collision of atoms and molecules in the surrounding environment. After above three physical processes, in fact, the OH radicals no longer involve the process of fluorescence radiation. Therefore, only a fairly small number of OH radicals can emit fluorescence from the excited state to the ground state. The physical process is shown in **Figure 1**.

The main purpose of the LIF technology is to determine the total number density of OH radicals by using the observable intensity of the OH fluorescence signal and then to obtain the local physical properties of the measured molecules. However, there are many physical processes difficult to observe directly in the LIF process, such as VET, RET, collisional quenching, and predissociation, which will greatly affect the intensity of the OH fluorescence signal. Therefore, if the concentration of fluorescence signal is directly obtained by observation, one will cause great deviation. Generally, the time scales of VET, RET, and collisional quenching effects are much less than the lifetime of OH fluorescence. Therefore, it is rather difficult to directly measure these physical processes on the OH fluorescence signal.

Under the linear excitation, the LIF signal intensity of the excited molecule in position x at atmospheric pressure can be expressed as follows [9]:

$$I_{\text{LIF}}(x, \omega, T, N_c) = \hbar\omega C_{exp} B_{mn} N_m^0 f_B(x, T) \frac{A_{nm}}{A_{nm} + Q(x, T, N_c)} \int_\omega \frac{I(x, \omega)}{c} g(x, \omega, T, N_c) d\omega \quad (1)$$
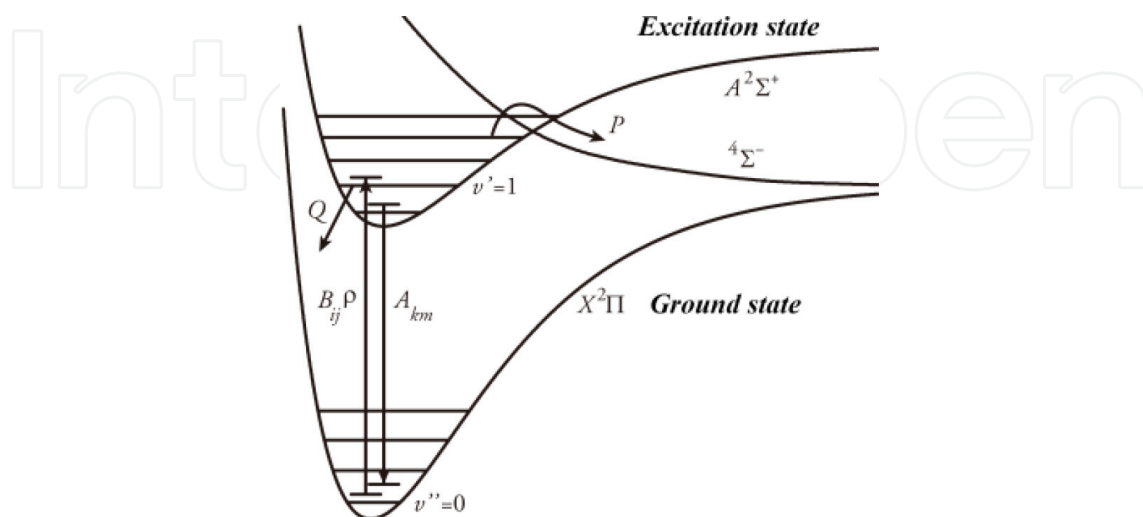

Figure 1. The LIF process of hydroxyl radical [9].

where $\hbar$ is the Planck reduced constant; ω is the angular frequency related to the energy interval between the selected excited levels; $C_{\exp}$ is an experimental constant influenced by the quantum efficiency of detector, the filter function, and the solid angle of optical system; B_{mn} is the Einstein stimulated absorption coefficient from low energy state (m state) to high energy state (n state); N_m^0 is the molecular number density in m state; $f_{\mathrm{B}}(x,T)$ is the Boltzmann Fraction in position x; T is the temperature; A_{nm} is the spontaneous emission rate of excited molecules transitioning from n state to m state; $Q(x,T,N_c)$ is the collisional quenching rate related to the temperature and the total number N_c around the collisional molecules; $I(x,\omega)$ is the intensity of excited laser in position x; and $g(x, \omega, T, N_c)$ is the molecular integrated absorption line-shape in position x. In Eq. (1), the factor of $A_{nm}/(A_{nm} + Q(x, T, N_c))$ represents the fluorescence quantum efficiency used to describe the percentage of fluorescence radiation energy in the total absorbed laser energy.

The actual OH energy-level structure is fairly sophisticated, so an approximate model of two energy levels is often used. Under the two energy-level approximation, the average collisional quenching rate Q is expressed as [9]

$$Q = \sum_i k_{Q_i} N_i \tag{2}$$

where N_i is the number density of the colliding particle ith and k_{Q_i} is the quenching rate coefficient of the colliding molecule ith, which can be expressed as

$$k_{Q_i} = \sigma_{Q_i} \langle v_i \rangle \tag{3}$$

where σ_{Q_i} is the collisional quenching cross section of the molecule ith and $\langle v_i \rangle$ is the average heat collisional speed of the colliding species ith, expressed as

$$\langle v_i \rangle = \sqrt{\frac{8 k_B T}{\pi \mu_i}} \tag{4}$$

where k_{B} is the Boltzmann constant and μ_i is the reduced mass of the colliding molecule ith.

As can be seen from Eq. (1), in order to determine the OH number density using observed LIF signals, it is necessary to exactly know all the factors impacting on the LIF signal, especially for the collisional quenching rate. For the premixed methane/air flame, the estimated average quantum yield is approximately 1/1000. This result shows that the effect of collisional quenching in flame is fairly strong and most of the OH radicals excited to the high energy state dissipate the absorbed laser energy in the form of non-radiative transition, such as collisional electronic quenching and VET. As a result, only a few OH radicals will release the absorbed energy to radiate fluorescence.

However, there are too many factors difficult to measure in the collisional quenching rate of OH radical in flames, including the quenching cross sections of colliding pairs, the average

heating collisional speed, and the number density of the collisional particles. It also can be seen from Eqs. (2)–(4) that it is rather difficult to determine the concentration, quenching section, and heating collisional speed of each collisional molecule accurately, because there are hundreds of species in the actual flame. Worse still, some colliding particles have the shorter life than OH radical, which leads to almost impossible to accurately determine the distributions of OH concentration in the observed location. In addition, the collisional environment of different flames varies also greatly. Even for only one kind of flame, the different working conditions will lead to a great change to the physical quantities affecting the rate of collisional quenching. Since there is little understanding about the non-radiative energy transfer processes of OH radical at present stage, it is almost impossible to measure the physical quantities, which can greatly affect the collisional quenching rate of OH radical by using the current experimental technique.

With the increasing demand for the spatial resolution of the internal structure of flame in the fields of combustion and aerodynamics, it is urgent to obtain the spatial distribution information for the combustion/flow fields, so as to further understand the basic characteristics of the chemical reaction in flames. PLIF is a laser diagnostic technique developed under this requirement, which is the expansion of LIF technology in two-dimensional space.

The physical process of PLIF is exactly the same as the LIF technology. The difference between PLIF and LIF is that the PLIF technique uses a special sheet-forming optics to replace the "line beam" used in the LIF by a "sheet beam." And the photomultiplier tube commonly used in LIF technology is replaced by an intensified charge-coupled device (ICCD) camera, which can make two-dimensional imaging for the weak fluorescence signal. The typical PLIF measuring system consists of five parts: the laser, the sheet-forming optics, the imaging acquisition and data storage, the digital delay control, and combustion systems, as shown in **Figure 2**.
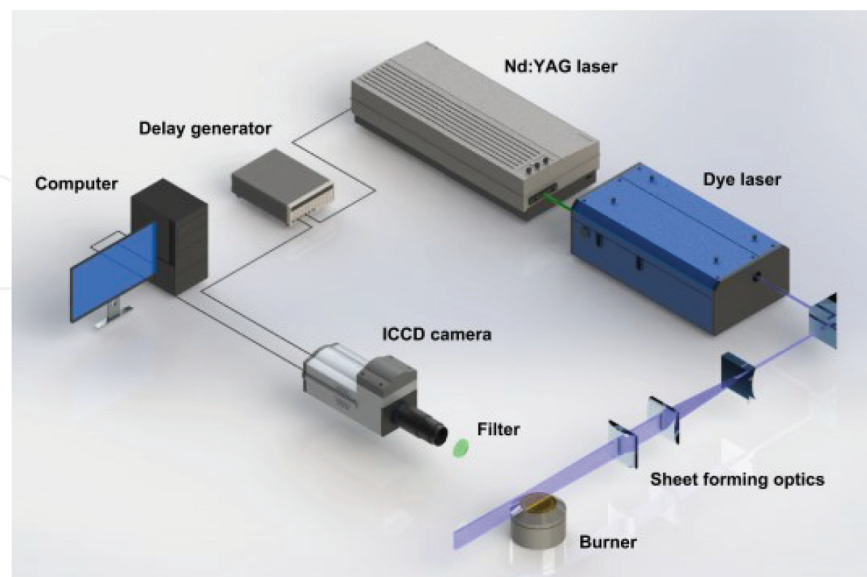

Figure 2. Typical PLIF experimental setup.

The laser source is usually composed of pump laser and dye laser to obtain a laser beam with different excitation wavelengths. The sheet-forming optics mainly consists of one cylindrical concave lens and other two vertical cylindrical convex lenses, achieving the transformation from line beam to sheet beam. The imaging acquisition and data storage system is mainly composed of ICCD camera and data storage module to acquire the weak fluorescence signals in a real time. The digital delay control system is used to control the synchronization between the laser and the ICCD camera. The burner is used to produce an objective flame to be researched. According to the characteristics of the actual research, the PLIF system will be slightly different, but the main assembly is still composed of the above five parts.

3. Review on the developments of the quantitative LIF

From the view of using purposes, LIF technology can be briefly divided into two categories: qualitative and quantitative. In this section, the current research status of quantitative LIF will be reviewed.

3.1. Calibration LIF

From Eq. (1), it is known that the following parameters should be measured accurately when using the PLIF image to deduce the concentration field of the species: the excitation laser wavelength, the experimental calibration constant, the Einstein stimulated absorption coefficient, the Boltzmann fraction, the fluorescence quantum yield (especially for the collisional quenching rate Q), and the convolution of the laser line shape and the molecular absorption line shape. However, it is difficult to obtain the exact values of the temperature, the fluorescence quantum yield, and other parameters at the same time in flames. Therefore, the quantification of the molecular concentration field is thought to be fairly difficult. In order to simplify the difficulty of quantification, calibrating these parameters with a standard flame, named calibration LIF, has been first proposed.

Using the calibration method to determine the species concentration field, the following simplification is needed: under the condition of linear excitation, it is considered that the concentration of the molecules to be measured is only related to the LIF signal intensity, calibration constant, flame temperature, and environmental pressure but independent of other factors. To further reduce the dependence of the Boltzmann fraction on temperature, it is always necessary to select an excited line, which is not sensitive to the changes of temperature. After the above simplification, it can be considered that the species concentration has a direct proportional relationship with the LIF signal intensity.

At present, extensive research for the measurements of the OH concentration spatial distribution has been studied by using the calibration LIF/PLIF. The typical research work is introduced as follows.

Arnold et al. [10] measured the OH concentration distributions in the premixed methane/air flame at pressures of 1, 5, and 20 bar by using the calibration LIF. The calibration factor was

obtained by ultraviolet (UV) absorption spectroscopy. Jalbert [11] researched the variations of OH concentration with the flame heights in the premixed methane/air and hydrogen/air flames. And the influences of the equivalent ratio and flow rate on the OH concentration have also been investigated by using the calibration LIF.

Although the calibration LIF has ability to measure the species concentration profiles to a certain extent, there is more serious problem that should not be neglected: the calibration LIF ignores the fact that the collisional quenching rates vary with the spatial position in the flame. Therefore, the calibration LIF cannot be considered as a real quantitative LIF strictly. It can only be regarded as a semiquantitative LIF technology.

3.2. Saturated LIF

When the excited energy density is higher than the threshold energy density of saturation excitation, the intensity of fluorescence signal is only related to the molecular number density, stimulated absorption, stimulated radiation, and spontaneous radiation but independent with excitation energy and the electronic quenching rate. This case is known as the saturated LIF.

In the saturated LIF, the measured fluorescence signal can directly reflect the number density of the stimulated molecules. The main drawback of the saturated LIF is that the output laser pulse is difficult to reach the required saturated excitation energy density. Therefore, it is difficult to achieve the planar concentration measurement for the species. In addition, because the laser pulse has a certain energy profile in time and space, it is easy to arise the so-called wing effect at the edge of energy profile. In other words, the laser energy density at the edge is less than the threshold energy density. Therefore, the excitation in this location still belongs to the linear excitation, leading to the fact that fluorescence signal is still affected by the collisional quenching effect. The researches on quantitative measurement of species concentration using saturated LIF mainly include:

Carter et al. [12] used saturated LIF to measure the OH concentration distributions in $C_2H_6/O_2/N_2$ flames under the high pressure. The experimental results indicate that the maximum OH concentration measured by saturated LIF is 1.10×10^{16}, 1.05×10^{16}, 1.18×10^{16} and 0.98×10^{16} molecules/cm^3, respectively, under the pressure of 0.98, 6.1, 9.2, and 12.3 atm.

Kohse-Höinghaus et al. [13] measured the concentrations of CH and OH radicals in a premixed C_2H_2/O_2 flames under the low pressure using saturation LIF. The experimental results show that the concentration of CH and OH radicals in acetylene/oxygen flame is 1.1×10^{13} cm^{-3} ($T = 1750 \pm 80$ K, height at 2.6 mm) and 8.9×10^{14} cm^{-3} ($T = 2000 \pm 100$ K, height at 7.5 mm), respectively, under the pressure of 13 mbar and the equivalence ratio of 1.2.

3.3. Laser-induced pre-dissociative fluorescence (LIPF)

LIPF has also been recognized a kind of quantitative LIF, which is proposed to solve the problem that the fluorescence signal is susceptible to collisional quenching effect in linear LIF. In the LIPF, the fluorescence quantum efficiency can be written as

$$\varphi = \frac{A_{nm}}{A_{nm} + Q(T, N_c) + P} \qquad (5)$$

where P represents the pre-dissociative rates of the molecules in the excited state.

Generally speaking, if the ground state molecules can be excited to a suitable upper level, then there is a relationship of $Q \ll P$. Taking the vibrational band (3,0) excitation of OH radical as an example, the typical spontaneous emission rate A in the upper level is approximately 1.6×10^4 s^{-1}, the collision quenching rate is about 10^9 s^{-1}, and the pre-dissociative rate is around at 1×10^{10} s^{-1}. Therefore, the effects of A and Q on the fluorescence quantum efficiency can be neglected. In the LIPF, it can be considered that the fluorescence quantum efficiency is only affected by the pre-dissociative effect, but has no obvious relevance with the spontaneous emission and the collisional quenching effects. If the calibration factor of LIF signal would be obtained by other methods (calibration or direct measurement), the measured molecular concentration in flames can be obtained by using this quantitative relationship.

Using LIPF to measure the concentration fields of the stimulated molecules can immunize the LIF signal from the interference of collision quenching effect and thus reduce the difficulty for the quantitative measurements. However, it will bring in another trouble that the higher dissociative rate will lead to the decrease of fluorescence quantum efficiency, which makes the fluorescence signal further weakened and difficult to capture. In addition, compared with the traditional linear LIF excitation wavelength, LIPF usually needs to excite the measured species to a higher excitation level. At the same time, the energy density of excitation laser should also be increased as high as possible, so as to meet a higher SNR requirement. These experimental conditions are rather incompetent for the common lasers. The researches on the quantitative concentration measurements using LIPF mainly include:

Yuan et al. [14] quantitatively measured the variations of the OH concentrations with the axial heights in a premixed methane/air and propane/air flat flames at the range of 1–5 atm and the equivalence ratio of 0.7–1.3. The experimental results indicate that the OH concentration in the methane/air flame reaches the peak at around 2 mm from the burner surface, with a numerical value of about 1.1×10^{16} molecules/cm^3. For propane/air flame, the peak OH concentration on the same conditions is much smaller than that of methane/air flames, with a value of about 1.5×10^{15} molecules/cm^3.

Brown et al. [15] measured the OH concentration profiles in a hydrogen/air diffusion flame using the LIPF and compared the experimental results with the numerical simulations. The experimental results show that the peak concentration of OH radical is 9.3×10^{16} molecules/cm^3 approximately in this flame.

3.4. Short-duration pulsed LIF

In the linear LIF, the duration of the excitation laser pulse (pulse width) is at the order of nanosecond, and the collision quenching rate is commonly 10^9–10^{10} s^{-1}, slightly less than the excited laser pulse width, while the fluorescence lifetime of the excited state molecules is around at a few nanoseconds. Therefore, if the nanosecond laser pulse is used to excite the molecules, and then the fluorescence emitted from excited molecules is collected by an ICCD camera with a

gate width of nanosecond, the detected fluorescence signals are bound to be seriously affected by the influence of electronic quenching effect. Nevertheless, if the picosecond or a shorter laser pulse is considered to use, the molecules will be distributed in the upper energy state before the collisional quenching occurs. In this moment, if the picosecond detector can be employed to collect the fluorescence emitting from the molecule, the fluorescence signal will no longer be influenced by the collisional quenching effect. This is known as the short-duration pulsed LIF.

Thus, the short-duration pulsed LIF is also a kind of quantitative LIF, which is independent of the collisional quenching effect. The shortcoming of short-duration pulsed LIF lies in the fact that it is difficult to output a laser beam with a pulse width of picosecond, and the gate width of ICCD camera is not easy to reach at the order of picosecond. Furthermore, as the laser pulse width and the gate width of the detector are all at the order of picosecond, the collected fluorescence signals will be relatively weak, and its SNR is extraordinary low, which are not convenient for practical engineering applications. The researches on quantitative measurements of species concentration using short-duration pulsed LIF mainly include:

Bormann et al. [16] used the single-pulse picosecond LIF to obtain the relative OH concentration profiles in a premixed stoichiometric CH_4/O_2 flame under the normal pressure. The experimental results indicate that the number of OH is exceedingly few in the preheating zone above the burner outlet. Most of the OH radicals are distributed near the flame front and the edge of the flame.

Brockhinke et al. [17] measured the OH concentration distributions in the hydrogen/air opposed diffusion flame using picosecond LIF and determined the concentration distributions of H atoms by three-photon LIF in the same flame. The experimental results suggest that the peak OH concentration is about 2.5×10^{16} molecules/cm^3 and the peak concentration of the H atom is around at 2.1×10^{16} molecules/cm^3 in the stagnation surface of diffusion flame.

3.5. Bidirectional LIF

Bidirectional LIF has been recognized as a non-calibration linear LIF, which is independent of the collisional quenching effect. In the bidirectional LIF, the number density of the stimulated molecules is only related to the effective peak absorption cross section of the measured molecules and the forward and backward fluorescence signals. It has no relevance with the collisional quenching effect, the calibration constant of the detection system, and the energy density of the excited laser. Using bidirectional LIF/PLIF to map the concentration distributions, the two laser beams (or sheet beams) propagating through flame in the opposite direction are required to excite the molecules in the flame, so as to obtain the forward and backward LIF/PLIF signals. With combining the effective peak absorption cross sections of the molecules by other measurement methods, the number density of the excited molecules can then be obtained.

The available literature shows that the embryonic form of the bidirectional LIF is first proposed by the Stepowski [18]. After that, Versluis et al. [8] have further developed it and given a more concise and explicit expression for the concentration measurements in the high absorptive flames. The first application of bidirectional LIF/PLIF to the quantification of the two-dimensional OH concentration distributions in a methane/oxygen torch flame is investigated by Versluis et al. Besides that, Brackmann et al. [19] also employed bidirectional LIF to achieve

the quantitative measurements of OH concentration distributions in an opposed diffusion flame. Because the opposed diffusion flame belongs to a kind of symmetrical flame, they used only one beam to excite the OH radicals and combined the mirror symmetry method to achieve the quantitative measurements of one-dimensional OH concentration distributions. Their experimental results indicate that the OH concentration is about 7.8×10^{15} molecules/cm^3 at the height of 1.8 mm from the burner nozzle. In addition, Tian et al. [20] also used bidirectional LIF to quantitatively measure the concentration of iron atoms in a premixed laminar propylene/oxygen/argon flat flames. However, the two opposite directional beams have not been employed in their experiments. Instead, the mirror symmetry method has been used to obtain the variations of the iron atom concentration with the axial heights.

Judging from the existing literature statistics, the current species concentration measurements based on bidirectional LIF/PLIF technology are still fairly scarce. Although the bidirectional LIF/PLIF has great advantages beyond other quantitative LIF/PLIF technologies, such as no collisional quenching effect, no special excitation conditions (e.g., large energy, short pulses, etc.) and no additional calibration, it has a high requirement for the spatial coincidence of the beams and the SNR of the fluorescence signal. In addition, the experimental expression of effective peak absorption cross section provided by Versluis et al. has a limitation, which is not applicable to the case of weak absorption. In view of this problem, we have supplemented and corrected the experimental measurement equation in this chapter. These difficulties have resulted in the fact that the research of species concentration measurement based on the bidirectional PLIF is almost at a standstill. Therefore, it is necessary to conduct the in-depth research in order to promote the further development of the bidirectional LIF/PLIF.

4. The fundamental theory of bidirectional LIF

4.1. Measurement equation of the species concentration profiles

A schematic of one-dimensional bidirectional LIF for molecular concentration measurement is shown in **Figure 3**. First we give a definition as described in the following. With ICCD camera for reference, the direction in which the laser beam traverses the flame from left to right is the backward direction, instead of reverse for the forward direction. The points $x = 0$ and $x = L$ denote the boundaries for the concentration calculation.

The laser-induced fluorescence signal intensity at the point x is given by the following expression:

$$F_b(x) = CS(x)\sigma_0 N(x)I_b(x) \tag{6}$$

where C is a constant depending on the collection angle of fluorescence signal and the detector sensitivity, $S(x)$ denotes the fluorescent quantum yield which is only dependent on the spontaneous emission rate and the collisional quenching rate $Q(x)$, σ_0 is the effective peak absorption cross section of molecules to be measured, and $N(x)$ represents the particle number density at point x. Consider a laser beam propagating through the flame at a fixed height from left to right along the x-axis in **Figure 1**. The beam will be attenuated according to the Lambert-Beer law, and the intensity is given by the following equation:
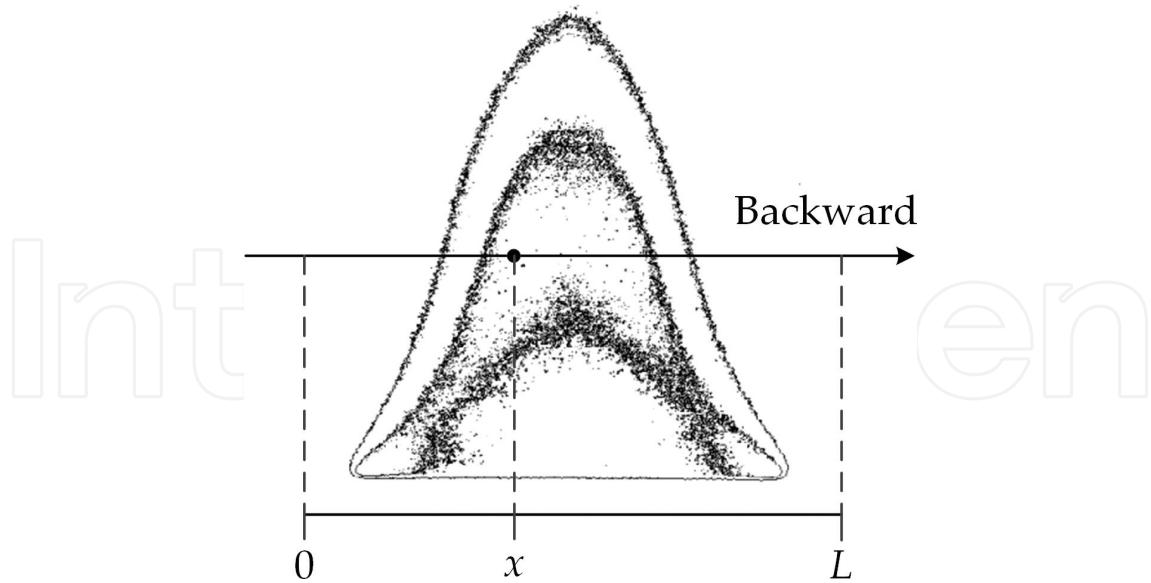
Figure 3. Schematic diagram for one-dimensional bidirectional LIF method.

$$I_b(x) = I_{b,0}e^{-\int_0^x \sigma_0 N(x)dy} \tag{7}$$

Eq. (7) is established in the unsaturated condition. In Eq. (7), $I_b(x)$ is the laser intensity in the backward direction at point x, and $I_{b,0}$ is the initial laser intensity of the backward beam at point $x = 0$. Similarly, if the laser propagates in the opposite direction from right to left, at the same height, the forward equation of the laser beam is given as

$$F_f(x) = CS(x)\sigma_0 N(x)I_f(x) \tag{8}$$

$$I_f(x) = I_{f,0}e^{-\int_0^x \sigma_0 N(x)dy} \tag{9}$$

where $I_f(x)$ is the laser intensity in the forward direction at point x and $I_{f,0}$ is the initial laser intensity of the forward beam. Note that the incident point of the forward beam is located at $x = L$. The ratio of fluorescence signals, $R(x)$, is equal to the ratio between the laser intensities because the factors of C, i.e., $S(x)$, σ_0, and $N(x)$, are canceled in the division expressed as

$$R(x) = \frac{F_f(x)}{F_b(x)} = \frac{I_f(x)}{I_b(x)} \tag{10}$$

Take the logarithm of the fluorescence ratio $R(x)$; then one will obtain the following equation:

$$\begin{aligned}\ln[R(x)] &= \ln\left[\frac{I_f(x)}{I_b(x)}\right] \\ &= \ln\frac{I_{f,0}}{I_{b,0}} + \int_0^x \sigma_0 N(y)dy - \int_x^L \sigma_0 N(y)dy \\ &= \ln\frac{I_{f,0}}{I_{b,0}} + 2\int_0^x \sigma_0 N(y)dy - \int_0^L \sigma_0 N(y)dy \end{aligned} \tag{11}$$

Finally taking the differential operation on Eq. (11), one can obtain

$$N(x) = \frac{1}{2\sigma_0} \frac{d}{dx} \ln \left[\frac{F_f(x)}{F_b(x)} \right] \tag{12}$$

which is a measurement equation of the species concentration profiles, representing the quantitative functional relationship between particle number density and LIF fluorescence intensity. Eq. (12) clearly shows that the particle number density is only associated with the forward and backward fluorescence intensities and the effective peak absorption cross section of particles under the linear excitation, independent of the temperature, pressure, quenching rate, laser energy, etc. It also suggests that the derivative of the fluorescence ratio $R(x)$ is very sensitive to noise in the LIF signal.

It is important to note that the $N(x)$ in Eq. (12) refers to the molecular number density in the excited level for the low rotational level J''. However, the total number density of the molecules to be measured N_0 is often concerned in the experiments. Therefore, it needs to be converted to N_0 after obtaining the experimental value of $N(x)$. In the state of thermal equilibrium, the relationship between the number density $N(v, J'', T)$ in the excited molecule and the total number density N_0 of the molecules is linked by the Boltzmann fraction $f_B(v, J'', T)$, and the mathematical expression is given as follows:

$$f_B(v, J'', T) = \frac{N(v, J'', T)}{N_0} = \frac{(2J'' + 1)}{Q_{vib} Q_{rot} Q_{elec}} e^{-(E_{vib} + E_{rot})/k_B T} \tag{13}$$

where k_B is the Boltzmann constant; T is the temperature; the vibrational quantum number J'' represents the rotational quantum number at the low energy level; E_{vib} and E_{rot} are vibrational and rotational energies, respectively; and Q_{vib}, Q_{rot}, and Q_{elec} are vibrational, rotational, and electronic partition functions, respectively.

Overall, the bidirectional LIF/PLIF is thought to be a no-calibration and no quenching effect LIF/PLIF technique, based on the combination of the traditional linear LIF/PLIF and absorption spectroscopy. It not only preserves the advantages of high spatial resolution of traditional LIF/PLIF but also absorbs the superiority of no quenching effect from absorption spectroscopy. It is of great significance to solve the problem of traditional quantitative LIF/PLIF technology.

4.2. Effective peak absorption cross section

From the view of the quantum mechanics, the absorption cross section describes the probability that the incident photon is absorbed by the target nucleus, and its unit usually has the dimension of area (cm^2). When the laser propagating along the x direction passes through the medium, the molecules will be attenuated by absorption, following the Lambert Bill absorption law. The differential form is expressed as

$$\frac{1}{I_{\bar{v}}(x)} \frac{dI_{\bar{v}}(x)}{dx} = -N(x)\sigma(\bar{v})P \tag{14}$$

where $I\overline{v}(x)$ is the intensity of laser at x point, v represents the wave number (cm^{-1}), P is the pressure (atm), $N(x)$ denotes the number density (cm^{-3}) of the excited molecules at the point x, and $\sigma(\overline{v})$ is the absorption cross section (cm^2) of the molecules. Eq. (14) is thought to be the phenomenological physical definition of the absorption cross section.

As long as the laser energy is not too high and the molecular number density is not too large, the absorption cross section can be considered directly proportional to the linear absorption function (cm) [21]:

$$\sigma(\overline{v}) = \sigma_{tot}g(\overline{v}) \tag{15}$$

where σ_{tot} is the integral absorption cross section (cm) and the line-shape function satisfies the normalization condition:

$$\int_{-\infty}^{\infty} g(\overline{v})d\overline{v} = 1 \tag{16}$$

To integrate Eq. (15), one can obtain

$$\sigma_{tot} = \int_{-\infty}^{\infty} \sigma(\overline{v})d\overline{v} \tag{17}$$

It can be seen that σ_{tot} is only related to the nature of the molecule but has no relationship with external environmental conditions. The integral absorption cross section is directly related to the oscillator strength of the molecule, with the expression of [22]

$$\sigma_{tot} = \frac{\pi e^2}{m_e c^2} f_{v'v''J'J''} \tag{18}$$

where e is the electronic charge (esu), m_e is the mass of electron (g), c is the speed of light (cm/s), and $f_{v'v''J'J''}$ is the molecular oscillator strength in the given oscillator transition, expressing as [23]

$$f_{v'v''J'J''} = \frac{f_{v'v''}(v',v'')}{4}\frac{S_{J'J''}}{2J''+1}T_{J'J''} \tag{19}$$

where v'' is the vibrational quantum number in the upper vibrational energy level; J'' is the vibrational quantum number in the lower vibrational level; is the vibrator strength, $S_{J'J''}$ is the rotational transition probability, that is, the Honl-London factor; and $T_{J'J''}$ represents the vibrational and rotational correction factor. The detailed values of $f_{v'v''J'J''}$, $S_{J'J''}$ and $T_{J'J''}$ can be found in the LIFBASE software.

In the actual experiment, the measured absorption line shape is not normalized, and thus

$$\int_{-\infty}^{\infty} \phi(\overline{v})d\overline{v} \neq 1 \tag{20}$$

For this reason, it is necessary to normalize it for obtaining the experimental expression of the effective peak absorption cross section.

The integral on the left side of Eq. (15) is defined as the relative integral absorption area *Int*. Normalizing above integral, one will obtain

$$\int_{-\infty}^{\infty} \frac{\phi(\overline{\nu})}{Int} d\overline{\nu} = \int_{-\infty}^{\infty} g(\overline{\nu}) d\overline{\nu} = 1 \tag{21}$$

Meanwhile, it is noted that if the first-term integral of Eq. (21) is multiplied on the left side of Eq. (17), one will get

$$\int_{-\infty}^{\infty} \sigma(\overline{\nu}) d\overline{\nu} = \sigma_{tot} \int_{-\infty}^{\infty} \frac{\phi(\overline{\nu})}{Int} d\overline{\nu} \tag{22}$$

That is

$$\sigma(\overline{\nu}) = \frac{\sigma_{tot} \phi(\overline{\nu})}{Int} \tag{23}$$

Eq. (23) is the relationship between the absorption cross section and the molecular absorption line profile measured experimentally.

In particular, if $\overline{\nu} = \overline{\nu}_0$, then

$$\sigma_0 = \sigma(\overline{\nu}_0) = \frac{\sigma_{tot} \phi(\overline{\nu}_0)}{Int} \tag{24}$$

where σ_0 is the effective peak absorption cross section; the numerical value of σ_{tot} can be calculated by Eq. (18). Eq. (24) is thought to be the experimental expression for measuring the effective peak absorption cross section of the molecule. Eq. (24) indicates that the effective peak absorption cross section of the molecule is related to the molecular absorption line shape and the relative integral absorption area.

As Versluis et al. have not clearly pointed out that the effective peak absorption cross section associates with the peak value $\phi(\overline{\nu}_0)$ of absorption line-shape, there is a difference between the effective peak absorption cross section and the actual value, if using the measurement equation given by Versluis et al. The difference is not obvious for the absorption band (0,0) of OH radical. However, this discrepancy will manifest significantly for the weak absorption band of (1,0). Therefore, the measurement equation of effective peak absorption cross section given by Versluis et al. is not applicable to the condition of weak absorption. To solve this problem, we revised the experimental equation. The corrected effective peak absorption cross section measurement equation is shown in Eq. (24). To confirm the validity of the modified measurement equation, the effective peak absorption cross section of the band (0,0) and band (1,0) within the $Q_1(8)$ line for the OH radical is measured, respectively. The experimental results show that the OH effective peak absorption cross section of the $Q_1(8)$ line for band (0,0) turns out to be about 5.5 times higher than that of band (1,0), while the theoretical calculation given by the LIFBASE simulation is about 6 times. The experimental result has been proven to be in good agreement with the simulation results.

5. Concentration profiles in a laminar flame by bidirectional PLIF

5.1. Measurements for the absolute OH concentration profiles in a partially premixed methane/air flat flame

The temperature distribution of $CH_4/O_2/N_2$ partially premixed flame is first measured by UV absorption spectrometry. The average temperature of the premixed flame of methane/air is 1772 K, with the statistical uncertainty of $\pm$10.4%. Then, the axial distributions of OH effective peak absorption cross section for $Q_1(8)$ line (the corresponding wavelength of 309.240 nm) in the band (0,0) are determined by using the wavelength scanning method. The statistical average of the OH effective peak absorption cross section on the axial direction is 1.10×10^{-15} cm^2 with the relative statistical uncertainty, which is $\pm$9.9%. The standard flat flame burner, designed by Hartung et al. [24], in the experiments is employed. More detailed experimental parameters can be found in the literature [25]. The variations of two-dimensional OH concentration fields with the equivalence ratios Φ (from 0.7 to 1.4) have been obtained in $CH_4/O_2/N_2$ partially premixed flat flame by using bidirectional PLIF, as shown in **Figures 4** and **5**.

Figures 4 and **5** show the two-dimensional spatial distributions of OH concentration in the methane/air partially premixed flame and its variations with the equivalence ratios, respectively. The actual size of each image is 15 mm $\times$ 46 mm, and the spatial resolution is 87.6 μm.

As can be seen from **Figure 4**, when the flame is burned in the lean-burn condition, the OH radicals are mainly distributed in a narrow band above the burner surface. With the increase of the axial distance, the OH concentration will decrease rapidly. On the other hand, the OH
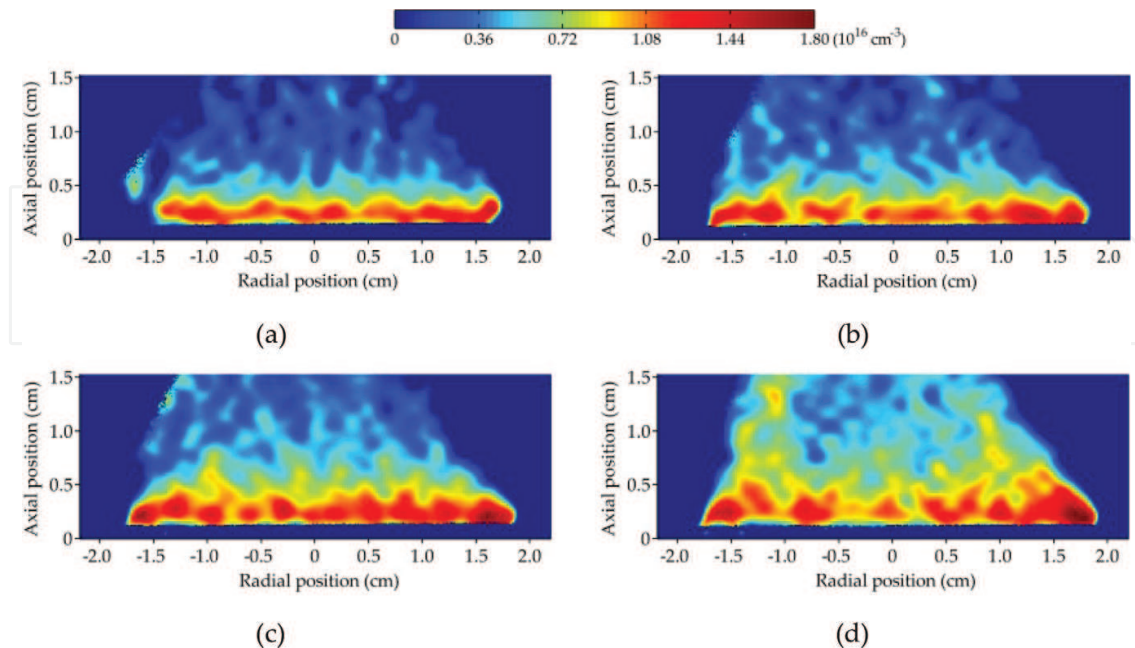

Figure 4. Variations of two-dimensional OH concentrations with equivalence ratios (Φ = 0.7–1.0). (a) Φ = 0.7, (b) Φ = 0.8, (c) Φ = 0.9, (d) Φ = 1.0.

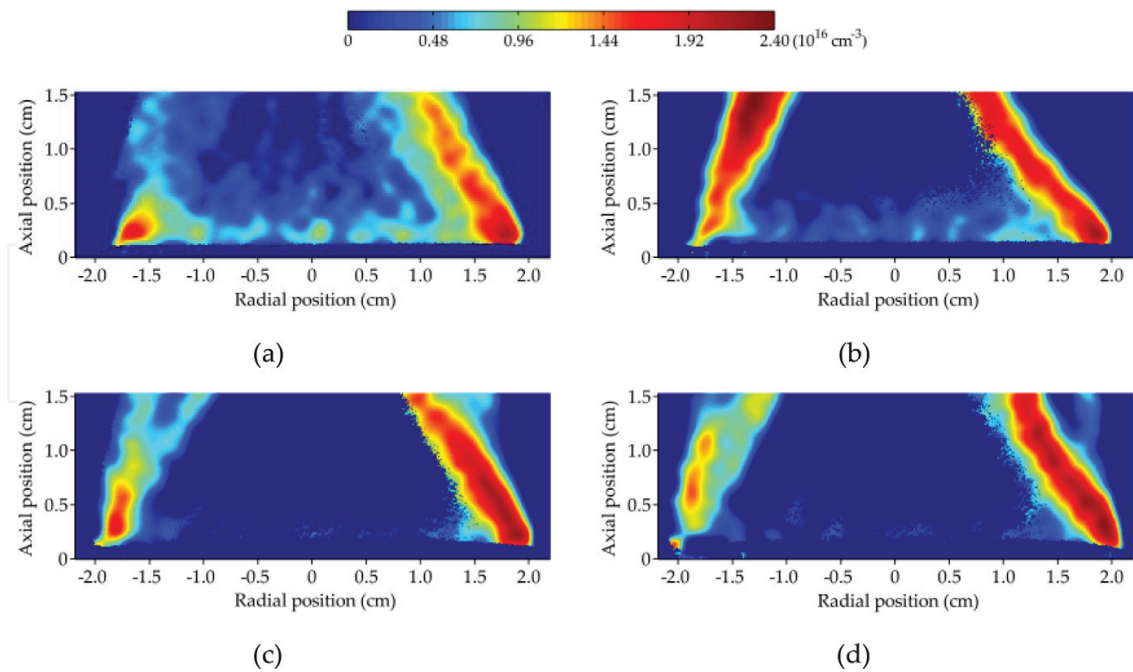**Figure 5.** Variations of two-dimensional OH concentrations with equivalence ratios (Φ = 1.1–1.4). (a) Φ = 1.1, (b) Φ = 1.2, (c) Φ = 1.3, (d) Φ = 1.4.

radical group gradually moves toward both sides of the flame, and the amount of OH radicals in the middle region is decreasing gradually with the increase of the equivalence ratio from 0.7 to 1. When the flame is burning at the rich-burn condition, as shown in **Figure 5**, the OH concentration profiles have changed greatly. That is, as the equivalence ratio continues to increase from 1.1 to 1.4, the two strong OH radical bands are formed on both sides of the flame. Meanwhile, the OH radical density in the middle region of flame decreases sharply.

5.2. Comparison between numerical simulation and experimental results

The comparison between the numerical simulations and the experimental results in the methane/air laminar partially premixed flame under different equivalence ratios is shown in **Figure 6**. The values of red translucency are the total uncertainties of the corresponding measured points.

From **Figure 6**, we can draw the following three conclusions:

1. In the range of equivalence ratio 0.7–1.2, the calculated results and the experimental values have the same variation trend with increasing the axial distance above the burner. The OH concentration increases rapidly to the maximum and then gradually decreases with the increase of axial distance, remaining unchanged at last. However, the experimental OH concentrations in the burnout zone decrease faster than the calculated results under certain equivalence ratios (e.g., equivalence ratios 0.8 and 0.9). The reason for this phenomenon mainly lies in the fact that the temperature results given by the GRI-Mech 3.0 mechanism are basically kept unchanged in this region, while the experimental temperature will decrease with increasing the axial distance.
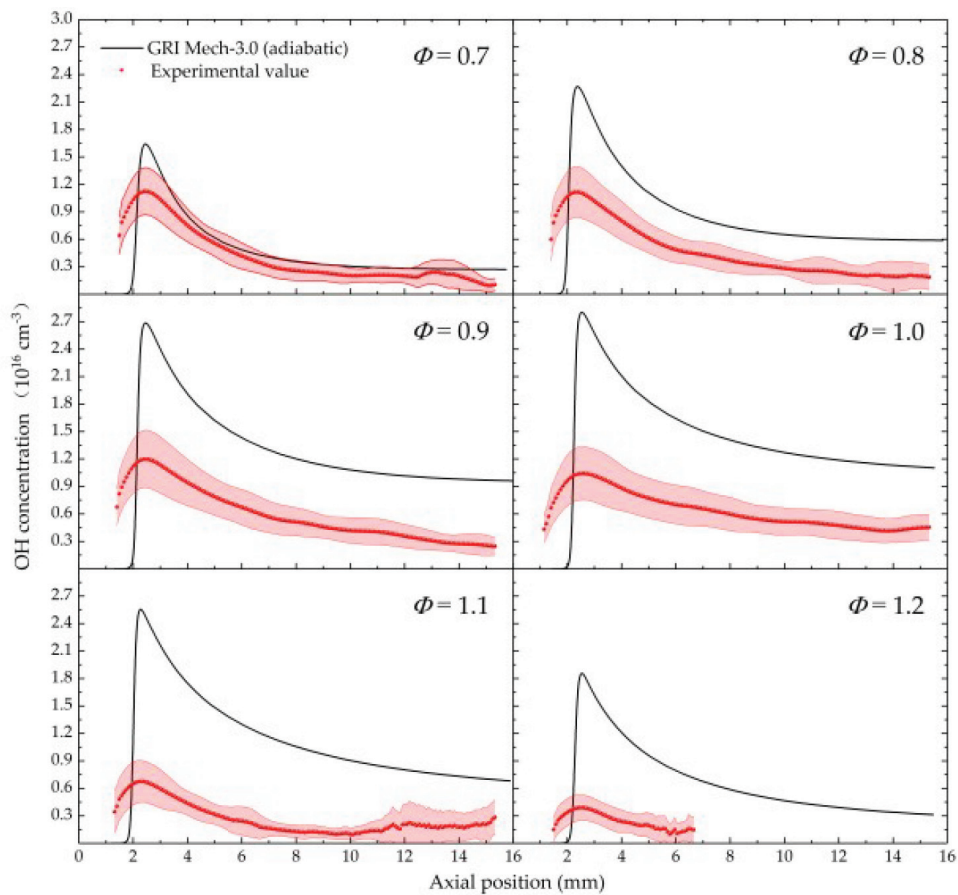
Figure 6. Comparison between experimental and numerical results of OH concentration in the central axis.

2. In the range of equivalence ratio 0.7–1.2, the calculated OH concentration is generally higher than the experimental values. It is not difficult to find that the OH concentration profiles based on the GRI-Mech 3.0 mechanism is in good agreement with the experimental variation trend only when the equivalent ratio equals to 0.7. The reason for the above difference may lie in the fact that the simulation gives the OH concentration distribution in the adiabatic state, but the actual flame is in a nonadiabatic state, and it is unavoidable to have some radiation loss. Therefore, the experimental measurement results of the OH concentrations are found to be always smaller than the corresponding calculation results. A rough calculation shows that the calculated temperature considering the radiation loss is about 150–250 K lower than that without taking into account the thermal radiation loss.

3. In the range of equivalence ratio 0.7–1.2, it is found that the OH concentration increases rapidly from zero to the maximum value. The experimental results indicate that the change speed of OH concentration is not as large as the calculated result and the measured OH concentrations are higher than the calculation results at the same axial position. It is presumed that the main reason for this phenomenon lies in the following: the width of the chemical reaction zone is rather narrow (about 1–2 mm) in the methane/air flat flame. When the flame reaches the stable combustion state, a large amount of heat will flow toward the burner surface and thus increase the flame temperature. Therefore, the temperature of the premixed gas inside the burner will be increased accordingly. As a consequence, the temperature of the
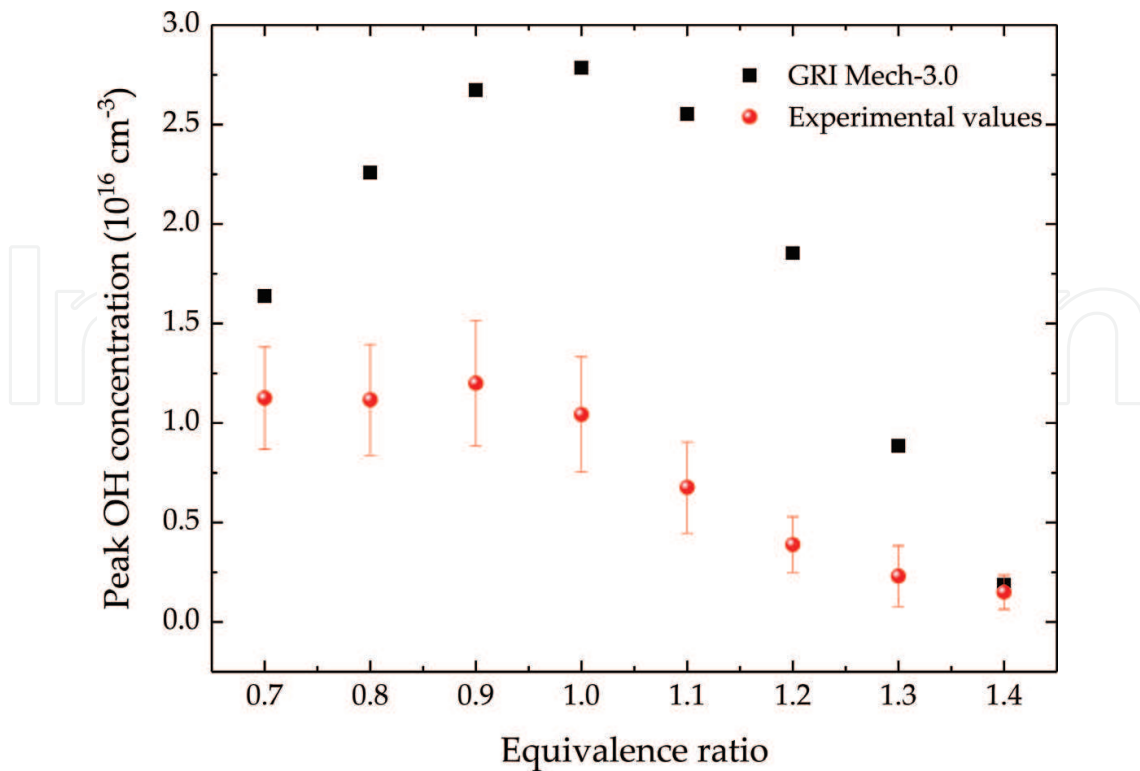
Figure 7. Comparison between experimental data and numerical simulation of peak OH concentration.

premixed gas will rise rapidly after flowing out from the burner and produce the chemical reaction, resulting in generating a large number of OH radicals. However, the temperature rising process of the premixed gas has not been taken into account in the numerical simulation. On the contrary, it is considered that the gas temperature near the outlet of burner is still in an ideal unheated state. Therefore, the measured OH concentrations are higher than the calculation results in the upstream of reaction zone.

The comparison results for the peak concentration under the conditions of different equivalence ratios have also been made, as shown in **Figure 7**. It can be clearly seen that the experimental results are smaller than the calculated values. The reason has already been analyzed before, so it is no longer mentioned here. Another notable phenomenon is that the measured OH concentration has not reached the maximum under the equivalent ratio of 1.0, but the peak OH concentration occurs in the lean-burn zone under the equivalence ratio of 0.9. The above experimental result indicates that even if the equivalence ratio of the premixed gas is set to 1.0, the fuel molecules still cannot be completely consumed in the actual combustion process. Therefore, we speculate that the OH reaction rate predicted by the simulation may be higher than the experimental value under the condition of stoichiometric ratio.

6. Conclusions

In conclusion, this chapter first reviews the developments of planar laser-induced fluorescence and briefly analyzes the existing problems of quantitative PLIF technology. Then, the advantages

and disadvantages of current quantitative PLIF technologies for species concentration measurements in flames are reviewed. And the latest works on the quantification of species concentration using PLIF in combustion are introduced. Thirdly, a non-calibration quantitative PLIF technology, named bidirectional PLIF, which is independent of collisional quenching effect, has been introduced in detail. As the current measurement equation of effective peak absorption cross section provided by Versluis et al. is found to be not applicable to the case of weak absorption, the revised experimental equation has been proposed in this chapter. At last, the two-dimensional spatial distributions of OH concentration and its variations with the equivalence ratios have been investigated in the methane/air partially premixed flame. The comparison between the experimental OH concentrations and the numerical simulation results has also been made under the equivalence ratios of 0.7–1.4. The result indicates that the OH concentration profiles measured by bidirectional PLIF are in good agreement with the predictive values performed by GRI-Mech 3.0 mechanism.

Acknowledgements

Author details

Zhen Yang[1,2,3]*, Xin Yu[1,2], Jiangbo Peng[1,2] and Jianlong Zhang[3]

*Address all correspondence to: sailoryz@163.com

1 National Key Laboratory of Science and Technology on Tunable Laser, Harbin Institute of Technology, Harbin, China

2 Institute of Opto-Electronics, Harbin Institute of Technology, Harbin, China

3 Institute of Optical Target Simulation and Test Technology, Harbin Institute of Technology, Harbin, China

References

[1] Hanson RK. Planar laser-induced fluorescence imaging. Journal of Quantitative Spectroscopy and Radiative Transfer. 1988;**40**(3):343-362. DOI: 10.1016/0022-4073(88)90125-2

[2] Xavier P, Vandel A, Godard G, et al. Investigation of combustion dynamics in a cavity-based combustor with high-speed laser diagnostics. Experiments in Fluids. 2016;**57**:50. DOI: 10.1007/s00348-016-2135-7

[3]   Elbaz AM, Roberts WL. Experimental study of the inverse diffusion flame using high repetition rate OH/acetone PLIF and PIV. Fuel. 2016;**165**:447-461. DOI: 10.1007/s00348-016-2135-7

[4]   Giezendanner-Thoben R, Meier U, Meier W, et al. Phase-locked two-line OH planar laser-induced fluorescence thermometry in a pulsating gas turbine model combustor at atmospheric pressure. Applied Optics. 2005;**44**(31):6565-6577. DOI: 10.1364/AO.44.006565

[5]   Seitzman JM, Hanson RK, DeBarber PA, et al. Application of quantitative two-line OH planar laser-induced fluorescence for temporally resolved planar thermometry in reacting flows. Applied Optics. 1994;**33**(18):4000-4012. DOI: 10.1364/AO.33.004000

[6]   Luque J, Jeffries JB, Smith GP, et al. Quasi-simultaneous detection of CH_2O and CH by cavity ring-down absorption and laser-induced fluorescence in a methane/air low-pressure flame. Applied Physics B. 2001;**73**(7):731-738. DOI: 10.1007/s003400100649

[7]   Luque J, Berg PA, Jeffries JB, et al. Cavity ring-down absorption and laser-induced fluorescence for quantitative measurements of CH radicals in low-pressure flames. Applied Physics B. 2004;**78**(1):93-102. DOI: 10.1007/s00340-003-1331-3

[8]   Versluis M, Georgiev N, Martinsson L, et al. 2-D absolute OH concentration profiles in atmospheric flames using planar LIF in a bi-directional laser beam configuration. Applied Physics B. 1997;**65**(3):411-417. DOI: 10.1007/s003400050289

[9]   Ehn A. Towards quantitative diagnostics using short-pulse laser techniques [thesis]. Lund: Lund University; 2012

[10] Arnold A, Bombach R, Käppeli B, et al. Quantitative measurements of OH concentration fields by two-dimensional laser-induced fluorescence. Applied Physics B. 1997;**64**(5):579-583. DOI: 10.1007/s003400050218

[11] Jalbert AM. A study of quantitative concentrations of hydroxyl (OH) in laminar flat flames using planar laser induced fluorescence (PLIF) [thesis]. Boston: Northeastern University; 2011

[12] Carter CD, King GB, Laurendeau NM. Saturated fluorescence measurements of the hydroxyl radical in laminar high-pressure $C_2H_6/O_2/N_2$ flames. Applied Optics. 1992;**31**(10):1511-1522. DOI: 10.1364/AO.31.001511

[13] Kohse-Höinghaus K, Heidenreich R, Just T. Determination of absolute OH and CH concentrations in a low pressure flame by laser-induced saturated fluorescence. Symposium on Combustion. 1985;**20**(1):1177-1185. DOI: 10.1016/S0082-0784(85)80606-8

[14] Yuan TH, Lai YH, Lu CJ, et al. Universal calibration of quantitative OH-LIPF measurements in hydrocarbon flames at elevated pressures. Combustion, Explosion, and Shock Waves. 2009;**45**(4):404-412. DOI: 10.1007/s10573-009-0050-4

[15] Brown TM, Tanoff MA, Osborne RJ, et al. Experimental and numerical investigation of laminar hydrogen-air counterflow diffusion flames. Combustion Science and Technology. 1997;**129**(1-6):71-88. DOI: 10.1080/00102209708935720

[16] Bormann F, Nielsen T, Burrows M, et al. Single-pulse collision-insensitive picosecond planar laser-induced fluorescence of OH $A^2\Sigma^+$ (v'=2) in atmospheric-pressure flames. Applied Physics B. 1996;**62**(6):601-607. DOI: 10.1007/BF01081698

[17] Brockhinke A, Bülter A, Rolon JC, et al. Ps-LIF measurements of minor species concentration in a counterflow diffusion flame interacting with a vortex. Applied Physics B. 2001; **72**(4):491-496. DOI: 10.1007/s003400100535

[18] Stepowski D. Local absorption measurement by laser-induced fluorescence. Applied Optics. 1987;**26**(9):1631-1635. DOI: 10.1364/AO.26.001631

[19] Brackmann C, Bood J, Aldén M, et al. Quantitative measurements of species and temperature in a DME-air counterflow diffusion flame using laser diagnostic methods. Combustion Science and Technology. 2006;**178**(6):1165-1184. DOI: 10.1080/00102200600582376

[20] Tian K, Li ZS, Staude S, et al. Influence of ferrocene dddition to a laminar premixed propene flame: Laser diagnostics, mass spectrometry and numerical simulations. Proceedings of the Combustion Institute. 2009;**32**(1):445-452. DOI: 10.1016/j.proci.2008.05.056

[21] Hilborn RC. Einstein coefficients, cross sections, f values, dipole moments, and all that. American Journal of Physics. 2002;**50**(11):982-986. DOI: 10.1119/1.12937

[22] McGee TJ, Mcilrath TJ. Absolute OH absorption cross sections (for lidar measurements). Journal of Quantitative Spectroscopy and Radiative Transfer. 1984;**32**(2):179-184. DOI: 10.1016/0022-4073(84)90082-7

[23] Anketell J, Pery-Thorne A. Oscillator strengths in the $^2\Sigma^+ \rightarrow 2\Pi$ dand system of OH by the hook method. Proceedings of the Royal Society A. 1967;**301**(1466):343-353. DOI: 10.1098/rspa.1967.0212

[24] Hartung G, Hult J, Kaminski CF. A flat flame burner for the calibration of laser thermometry techniques. Measurement Science and Technology. 2006;**17**(9):2485-2493. DOI: 10.1088/0957-0233/17/9/016

[25] Zhen Y, Xin Y, Peng J, et al. Quantitative measurements of one-dimensional OH absolute concentration profiles in a methane/air flat flame by bi-directional laser-induced fluorescence. Chinese Physics B. 2015;**24**(11):114204. DOI: 10.1088/1674-1056/24/11/114204